Available online at www.sciencedirect.com
SCIENCE DIRECT
ELSEVIER
Journal of the European Ceramic Society 26 (2006) 1473–1479
ECERS
www.elsevier.com/locate/jeurceramsoc

EELS characterisation of β-tricalcium phosphate and hydroxyapatite

Giuliano Gregori [a,*], Hans-Joachim Kleebe [b], Helmar Mayr [a], Günter Ziegler [a]

[a] *University of Bayreuth, Friedrich Baur Research Institute for Biomaterials, Ludwig-Thoma Straße 36C, D-95447 Bayreuth, Germany*
[b] *Colorado School of Mines, Metallurgical and Materials Engineering Department, Golden, CO 80401, USA*

Received 8 September 2004; received in revised form 18 January 2005; accepted 12 February 2005
Available online 12 April 2005

Abstract

Hydroxyapatite (HA) and β-tricalcium phosphate (β-TCP) are of great interest due to their potential application as bone-replacement materials. In particular, composites made of a mixture of these Ca-phosphates revealed improved mechanical properties; however, the reason for this improvement is unknown. Future development and properties enhancement of such bioceramics is linked to the possibility to characterise their particular microstructure. In this context, the ability to quickly identify individual grains of HA and β-TCP within these composites will allow acquiring information about the phase distributions and the phase-boundary microstructure. The aim of the present study is, therefore, to demonstrate that electron energy-loss spectroscopy (EELS) can be successfully employed to differentiate between individual grains of HA and β-TCP. In particular, the analysis of the near-edge structure of the oxygen *K*-ionisation edge allows detection of a characteristic signal at ca. 536 eV that can be employed as an identification tool for HA. EELS investigations were performed first on as-received and calcined (1000 °C) HA and β-TCP powders and subsequently on pure bulk HA and β-TCP samples sintered at 1250 °C. Finally, this method was successfully applied to a HA/β-TCP (50/50 wt.%) composite sintered at 1250 °C.

Keywords: Apatite; Tricalcium phosphate; Electron microscopy; Biomedical applications

1. Introduction

Synthetic β-tricalcium phosphate (β-TCP), $Ca_3(PO_4)_2$, and hydroxyapatite (HA), $Ca_{10}(PO_4)_6(OH)_2$, are compounds with a high potential for bioapplications. In particular, composites made of β-TCP and HA, so-called biphasic calcium phosphates (BCPs), which combine the excellent bioactivity of HA with the good bioresorbability of β-TCP, are interesting candidates for medical applications as, for example, materials for bone replacement.[1–3]

One main motivation for the present study is the reported improvement of the resulting mechanical properties of bulk BCPs, as compared to pure HA or β-TCP components.[4–6] Raynaud et al.[6] showed that a BCP containing 10 wt.% of β-TCP exhibits double tensile strength compared to pure HA ceramics. The comprehension of the factors that rule this improvement and, therefore, the further enhancement of the mechanical properties of such composites is strongly linked to the characterisation of the corresponding microstructure. Since β-TCP and HA have similar stoichiometry (see Table 1), one of the main limitations in the study of BCP composites is presently the difficulty to identify the different phases (β-TCP versus HA) within the microstructure. In general, an experimental technique allowing the fast recognition of single grains is essential for understanding the morphology and the distribution of the two phases. Importantly, the ability to quickly distinguish single grains is also a prerequisite for the characterisation of the interface between grains of the two different phases.

Transmission electron microscopy (TEM) offers the possibility to perform high-resolution imaging, diffraction as well as local chemical analysis with high lateral resolution. Energy dispersive X-ray analysis (EDX),[7,8] convergent beam electron diffraction (CBED),[9] and high-resolution TEM (HRTEM)[9,10,13–15,17] have been used to characterise

* Corresponding author. Present address: California NanoSystems Institute, University of California, Santa Barbara, CA 93106-6105, USA. Tel.: +1 805 893 8138; fax: +1 805 893 6132.
E-mail address: giuliano@engineering.ucsb.edu (G. Gregori).

0955-2219/$ – see front matter © 2005 Elsevier Ltd. All rights reserved.
doi:10.1016/j.jeurceramsoc.2005.02.007

Table 1
Stoichiometry and crystallographic data of β-tricalcium phosphate and hydroxyapatite

Material	Stoichiometry	Crystallographic symmetry	Lattice parameters (Å)
β-Tricalcium phosphate	$Ca_3(PO_4)_2$	Rhombohedral (*R*3*c*)	$a = 10.43$; $c = 37.39$
Hydroxyapatite	$Ca_{10}(PO_4)_6(OH)_2$	Hexagonal ($P6_3/m$)	$a = 9.43$; $c = 6.87$

various calcium phosphate materials. Kleebe et al.[9] showed that after sintering at 1250 °C, undoped HA exhibited a homogeneous microstructure with approximately 4% residual porosity. HRTEM characterisation revealed the presence of a very small, disordered interface region, also denoted as extended grain-boundary structure. The absence of any intergranular glass film suggested that densification proceeded without the formation of a liquid phase. Brès et al.[10] performed high-resolution TEM investigations on human tooth enamel and different synthetic calcium phosphates. Energy-filtered TEM was employed by Arnold et al.[11] to investigate the early stages of crystal formation in dentine, bone, enamel and natural apatite. They found that the early crystallites exhibit a para-crystalline character, similar to the structure observed in biopolymers. Leng et al.[12] employed bright-field imaging and electron diffraction to characterise precipitates which appeared on the surface of biphasic calcium phosphates upon in vitro and in vivo experiments.

However, the above-mentioned methods are not well suited for the local identification of HA versus β-TCP in biphasic calcium phosphate composites. Since the value of the Ca/P atomic ratio in the two systems is rather close (1.67 for HA and 1.5 for TCP), EDX analysis cannot be utilised because the accuracy of this technique is insufficient (in addition to the experimental problem of electron beam induced cation migration).

With respect to CBED, the method can be applied for the identification of adequately oriented grains, but presents the drawback of a rather long and elaborated analysis of the electron diffraction data. As far as HRTEM is concerned, it should be noted that the electron beam irradiation can induce significant damages to calcium phosphate compounds. Brès et al.[13] observed that the human dental enamel underwent significant modifications under the TEM electron beam and observed the beam-induced formation of CaO. According to Nicolopoulos et al.[14] the electron beam induces compositional as well as microstructural variations in HA compounds, which can be related to a hexagonal-to-monoclinic phase transformation. Meldrum et al.[15] investigated the effect of electron irradiation on crystalline and amorphous apatites. They showed that the TEM electron beam induced the decomposition of the starting HA crystals through a dehydration process yielding the precipitation of cubic CaO. It was shown that beam current density and temperature were competing parameters in the formation process of CaO. Typically, the HA crystal structure is assigned to the hexagonal space group $P6_3/m$[9,16] however, the analysis of HRTEM micrographs performed by Henning et al.[17] revealed *P*3 projection symmetry along [0 0 1] in several HA grains, which is not compatible with the hexagonal space group. The authors correlated the reduced threefold symmetry with the dehydration process of hydroxyapatite occurring under the electron beam.

The present study is performed with the aim of showing that electron energy-loss spectroscopy (EELS) can be employed in order to quickly and precisely distinguish between HA and β-TCP grains in biphasic calcium phosphate composite.

Here, the technique allows the identification of single grains in a BCP composite having an average grain size of few microns, but the method can be successfully used for the characterisation of grains also at submicron scale.

2. Experimental

The samples used in the present study were prepared starting from pure β-TCP and HA powders produced by the company Merck, Germany. The composition of the β-TCP powder provided by Merck corresponds to a calcium-deficient

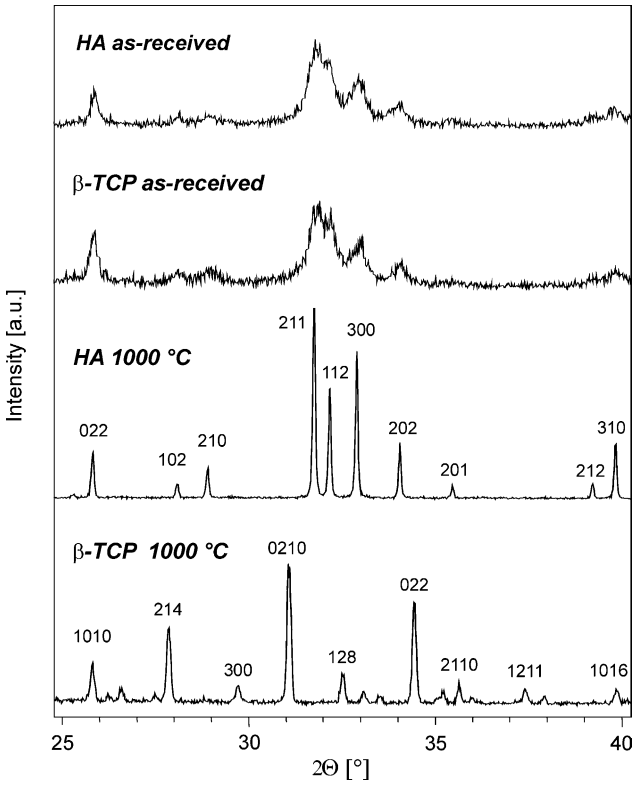

Fig. 1. XRD patterns of HA and β-TCP powders "as received" and after thermal treatment at 1000 °C.

HA, which undergoes the following reaction[18]

$$Ca_9(HPO_4)(PO_4)_5(OH) \rightarrow 3Ca_3(PO_4)_2 + H_2O \quad (1)$$

during thermal treatments at temperatures ranging between 700 and 900 °C, yielding the formation of pure β-TCP.

As-received as well as powders calcined at 1000 °C for 1 h in air were investigated. In addition, bulk samples were prepared from the same starting powders, as follows: the powders were first heat-treated at 700 °C for 1 h and then added to a butanolic solution of wax, polyethylenglycol (PEG) and butanediol. The suspension was stirred for 30 min and subsequently dried in a rotational vacuum dryer. After sieving to <0.5 mm, the powders were granulated in a tubular mixer for 1 h. The resulting granulate was uniaxially pressed at 80 MPa and the so-obtained discs (30 mm diameter and approximately. 1 mm thickness) were sintered at 1250 °C for 1 h in air with a heating rate of 450 °C/h. These sintering parameters yield dense samples (99% of the theoretical density for HA and 97% for β-TCP) while remaining below the temperature (ca. 1300 °C) at which the β-TCP starts to transform into α-TCP (compare also the X-ray diffraction (XRD) plots shown in Figs. 1 and 4).

In order to prepare TEM powder specimens, HA or β-TCP powders were dispersed in acetone using an ultrasonic bath for 5 min. Few drops of the suspensions were then placed on holey carbon coated Cu-grids. With respect to bulk specimens, the preparation of TEM-foils, starting from the sintered monoliths, was achieved by standard ceramographic techniques: cutting, ultrasonic drilling, dimpling and Ar-ion thinning to perforation, followed by thin carbon coating to avoid electrostatic charging under the electron beam.

The samples were investigated using a transmission electron microscope Philips CM20 FEG (field emission gun) operating at the acceleration voltage of 200 kV. The microscope is equipped with a parallel electron energy-loss spectrometer (PEELS), model 666 (Gatan Inc.). In order to reduce the Boersch effect, the extraction voltage of the FEG was set at 3.5 kV, which corresponds to an emission current of <50 μA. During the analysis, a 200 μm SAD aperture was inserted to block the non-collimated electrons that can result from the electron scattering process in the electron gun. All spectra, collected

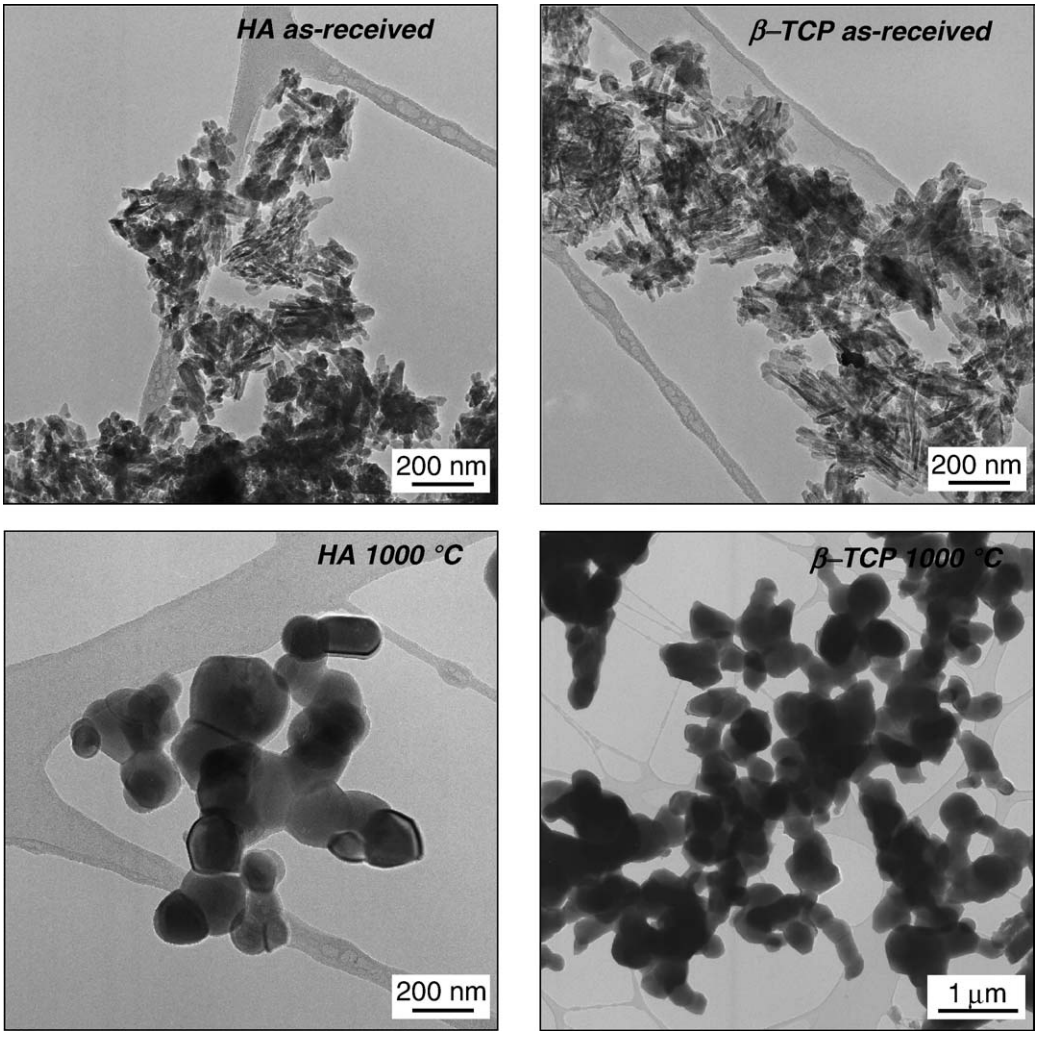

Fig. 2. TEM bright-field micrographs of β-TCP and HA powders "as received" and heat-treated at 1000 °C.

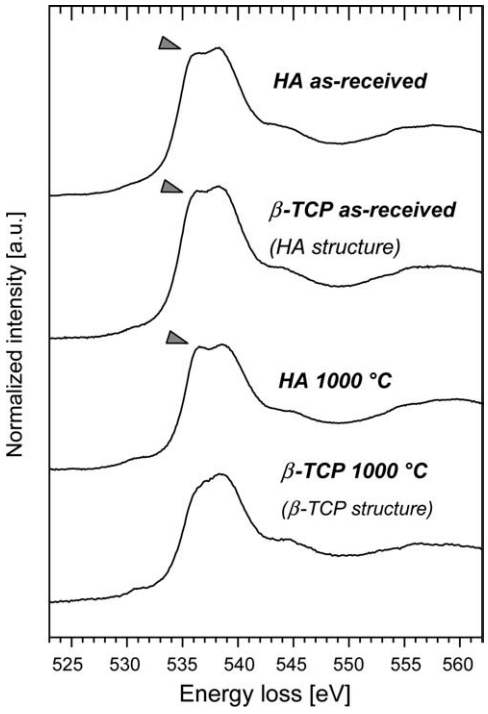

Fig. 3. EELS oxygen *K*-ionisation edge spectra acquired from β-TCP and HA powders "as received" and heat-treated at 1000 °C. To note the change in the β-TCP spectra.

from areas having a diameter of approximately 150 nm, were acquired with the 2 mm PEELS entrance and with an energy dispersion of 0.1 eV/channel. The energy resolution, defined as the full width at half maximum of the zero-loss peak, was ca. 0.8 eV.

A Gatan cooling holder model 613 coupled to a power supply model 613-0500 was employed in order to minimise possible microstructural changes due to the electron beam radiation.[13–15] The cold stage was filled with liquid nitrogen and the measurements were carried out only when the temperature stabilised (approximately 100 K). The experimental data were subsequently elaborated using the software EL/P 3.0 (Gatan Inc.).

EELS spectra at the oxygen *K*-ionisation edge (O_K-edge) were collected from different HA and β-TCP samples as well as from a HA/β-TCP composite. Preliminary measurements involved also the analysis of the phosphorus and calcium *L*-edges, but since the most remarkable results were obtained from the O_K-edge, the present study focuses on these data.

3. Results and discussion

The purity of the starting powders was first verified by X-ray diffraction analysis using a Seifert 3000P diffractometer with Cu Kα radiation. XRD patterns acquired from as-received as well as calcined (1000 °C) powders are shown in Fig. 1. The spectra obtained from both as-received powders are virtually identical, confirming that the TCP powder pro-

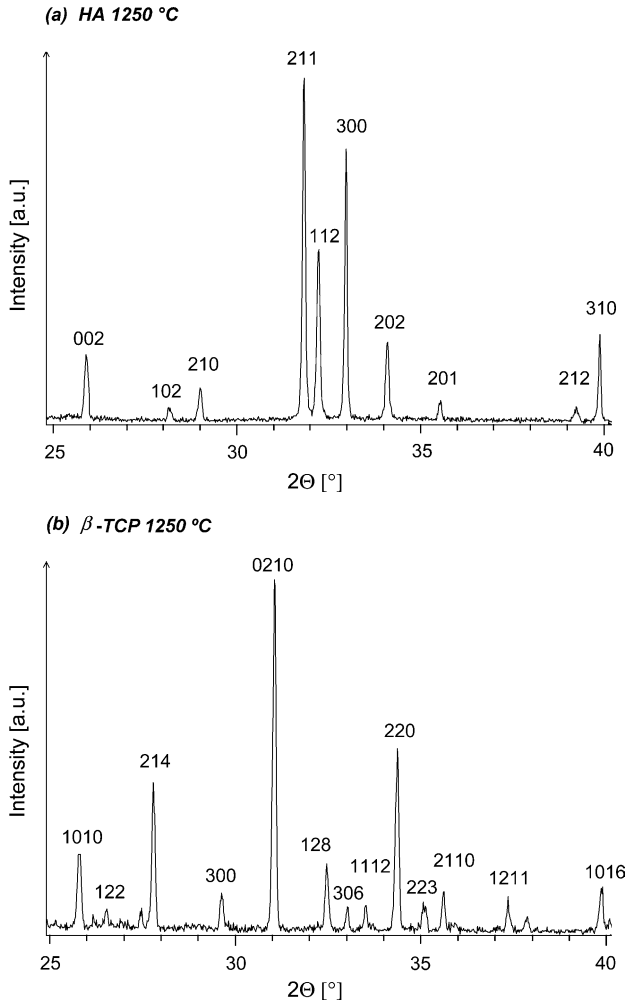

Fig. 4. XRD patterns of pure (a) HA and (b) β-TCP bulk samples upon sintering at 1250 °C.

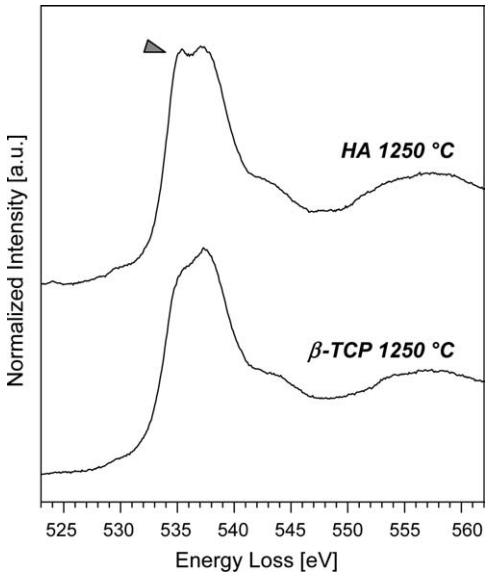

Fig. 5. EELS oxygen *K*-ionisation edge spectra of β-TCP and HA bulk samples sintered at 1250 °C.

vided by Merck consisted in fact of a calcium-deficient HA powder. Thermal treatment at 1000 °C induces the sintering process, as illustrated in the bright-field TEM micrographs given in Fig. 2. XRD data collected from the calcined powders exhibited different peak positions, which, according to JCPDS cards 09-0432 and 09-0169, could be assigned to pure HA and β-TCP (compare also Eq. (1)).

EELS O_K-ionisation edge analysis was performed on these powders, and the corresponding experimental spectra are shown in Fig. 3. All spectra are characterised by the presence of two major signals centred at about 538 and 557 eV. In addition, a weak pre-peak located at ca. 531 eV as well as a shoulder at approximately 544 eV can be observed at all O_K-edges. The spectra collected from the as-received powders are virtually identical. In particular, a more detailed analysis of the near-edge structure of these spectra allows to recognize the presence of two distinct signals superimposed on the main peak which are located at ca. 536 and 539 eV. Importantly, these signals are also present in the data recorded from HA powders exposed at 1000 °C but not in the spectrum of β-TCP where the superimposed feature around 536 eV is absent.

These first results indicate that the analysis of the EELS O_K-edge allows the identification of different calcium phosphate powders after calcination, simply by acquiring in few seconds an EELS spectrum and confirming the absence or presence of the small feature at 536 eV. This method was then employed to investigate a set of bulk samples of pure HA and β-TCP sintered at 1250 °C. Before performing EELS, the samples were characterized by XRD analysis to verify the phase purity of both systems. The corresponding experimental spectra are shown in Fig. 4. Besides the identification of the two components, the XRD spectra also indicate that: (i) neither the hydroxyapatite phase started to decompose and (ii) nor the β-to-α transformation of TCP occurred during sintering at 1250 °C.

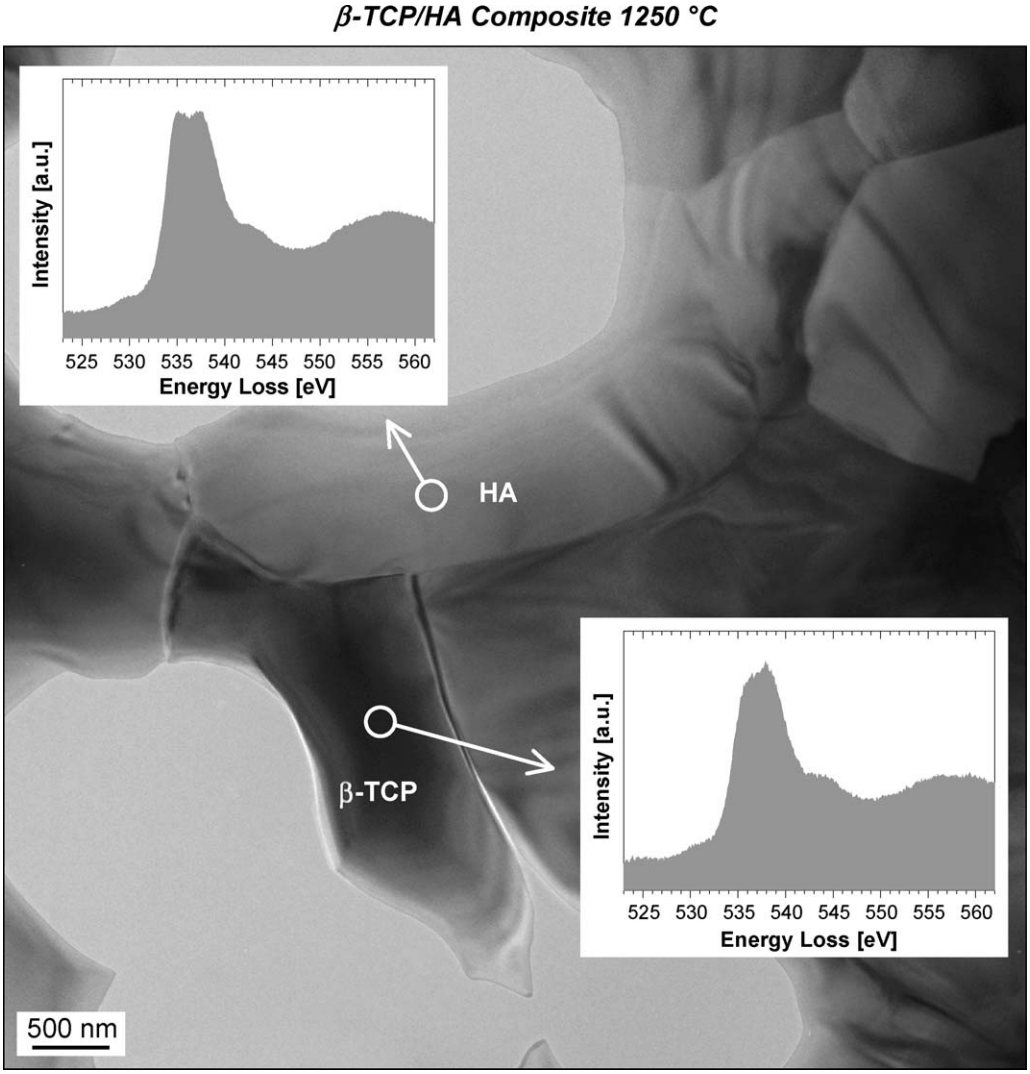

Fig. 6. TEM bright-field micrograph of the β-TCP/HA composite exposed at 1250 °C. The insets show the corresponding EELS oxygen *K*-edge spectra obtained from two distinct grains. The white circles represent the size of the electron beam during the analysis (diameter = 150 nm).

Numerous EELS spectra were acquired from bulk HA and β-TCP samples. Representative spectra for each material are shown in Fig. 5. Importantly, while β-TCP exhibits an asymmetric peak with a maximum at ca. 538 eV, HA is characterised by a splitting of the main signal, which results in two distinct peaks centred at ca. 536 and 539 eV. This confirms that EELS analysis can be used as an effective tool for the recognition of HA versus β-TCP phase. The goal of the present study was to prove that this method can be employed to individually identify each of the two compounds in a biphasic composite. For this reason, a 50/50 wt.% β-TCP/HA mixture was sintered at 1250 °C and subsequently analysed via EELS. The results given in Fig. 6 clearly confirm that the EELS O_K-edge investigation can be used to unequivocally identify individual grains. Here, the average size of the composite grains is few microns but the diameter of the areas exposed to the electron beam during the EELS analysis were 150 nm large, as illustrated by the white circles in Fig. 6 (see also Section 2).

The acquisition of spectra from smaller areas can be accomplished provided that the longer exposure time required to maintain a good signal-to-noise ratio does not induce the degradation of the sample under the electron beam. Based on our experience, the technique can be successfully employed also for the investigation of composites having grain size at submicron scale, e.g., diameter = 100 nm, as long as a cold stage is employed.

From the experimental data obtained in the present study we can conclude that the signal located at ca. 536 eV can be considered as a chemical fingerprint of the oxygen atoms present in the HA structure. This result indicates that the electronic structure of oxygen in HA is characterised by the presence of additional electronic states above the Fermi energy level compared to the oxygen sites present in β-TCP (see the additional peak at 536 eV). It is assumed that these additional states are due to the presence of OH-groups (or oxyl-groups), which are expected to be present in the HA structure (even after exposure at 1250 °C) according to the results of the thermo-gravimetric analysis shown in Fig. 7. Here, the experimental data indicate that the weight-loss due to the emission of H_2O proceeds above 1250 °C.

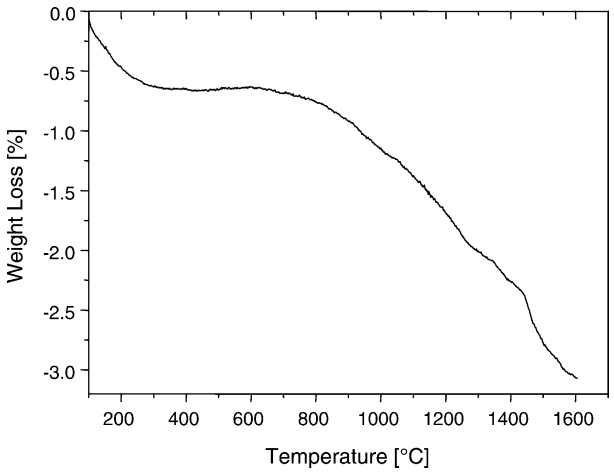

Fig. 7. Thermo-gravimetric analysis of HA.

Hence, the additional signal at the O_K-ionisation edge is related to the different crystal structures of the two compounds (Table 1).[19–22] The crystal symmetry of β-TCP is rhombohedral and its microstructure consists of Ca-cations and PO_4 tetrahedral units. Note that all oxygen atoms present in the β-TCP structure are confined to the PO_4 tetrahedra. In HA instead, hydroxyl (or oxyl) groups are present in addition to the PO_4 units and Ca-cations, giving rise to additional oxygen sublattice sites, as compared to β-TCP. These are responsible for the different electronic environments detected by EELS.

This work proves that EELS can be used to quickly and unequivocally identify HA and/or β-TCP grains, which is a prerequisite for further studies on the cause of the observed variations of the mechanical properties of HA/β-TCP composites.

4. Conclusions

The present study convincingly shows that EELS analysis can be employed to identify the electronic structure of individual grains present in β-TCP/HA composites. In particular, the presence of an additional signal at the oxygen ionisation edge (at ca. 536 eV) can be considered as a unique chemical fingerprint for the identification of HA versus β-TCP. The slightly different near-edge structure of the O_K-ionisation edge is closely related to the respective crystal structures of HA and β-TCP, in particular, to the different oxygen sublattice sites present in HA, as compared to β-TCP.

This work shows also that EELS analysis is well suited for the recognition of different calcium phosphate phases also at submicron scale.

Acknowledgements

The authors are grateful to Dr. F. Langenhorst (Bayerisches Geoinstitut, University of Bayreuth, Germany) for helpful discussions. The German Science Foundation (DFG) is thanked for the financial support (contract Zi 275/27-1) throughout this project.

References

1. Suchanek, W. and Yoshimura, M., Processing and properties of hydroxyapatite-based biomaterials for use as hard tissue replacements implants. *J. Mater. Res.*, 1998, **13**, 94–117.
2. Gauthier, O., Bouler, J.-M., Aguado, E., LeGeros, R. Z., Pilet, P. and Daculsi, G., Elaboration conditions influence physicochemical properties and in vivo bioactivity of macroporous biphasic calcium phosphate ceramics. *J. Mater. Sci.: Mater. Med.*, 1999, **10**, 199–204.

3. Bohner, M., Physical and chemical aspects of calcium phosphates used in spinal surgery. *Eur. Spin. J.*, 2001, **10**, 114–121.
4. Raynaud, S., Champion, E., Bernache-Assollant, D. and Thomas, P., Calcium phosphate apatites with variable Ca/P atomic ratio. I. Synthesis, characterisation and thermal stability of powders. *Biomaterials*, 2002, **23**, 1065–1072.
5. Raynaud, S., Champion, E. and Bernache-Assollant, D., Calcium phosphate apatites with variable Ca/P atomic ratio. II. Calcination and sintering. *Biomaterials*, 2002, **23**, 1073–1080.
6. Raynaud, S., Champion, E., Lafon, J. P. and Bernache-Assollant, D., Calcium phosphate apatites with variable Ca/P atomic ratio. III. Mechanical properties and degradation in solution of hot pressed ceramics. *Biomaterials*, 2002, **23**, 1081–1089.
7. Takadama, H., Kim, H.-M., Kokubo, T. and Nakamura, T., TEM–EDX study of process of apatite formation on bioactive titanium metal in simulated body fluid. *Key Eng. Mater.*, 2001, **192–195**, 51–54.
8. Bouler, J.-M. and Daculsi, G., In-vitro carbonated apatite precipitation on biphasic calcium phosphate pellets presenting various HA/β-TCP ratios. *Key Eng. Mater.*, 2001, **192–195**, 119–122.
9. Kleebe, H.-J., Brès, E. F., Bernache-Assollant, D. and Ziegler, G., High-resolution electron microscopy and convergent-beam electron diffraction of sintered undoped hydroxyapatite. *J. Am. Ceram. Soc.*, 1997, **80**, 37–44.
10. Brès, E. F., Moebus, G., Kleebe, H.-J., Pourroy, G., Werkmann, J. and Ehret, G., High resolution electron microscopy study of amorphous calcium phosphate. *J. Cryst. Growth*, 1993, **129**, 149–162.
11. Arnold, S., Plate, U., Wiesmann, H. P., Stratmann, U., Kohl, H. and Höhling, H. J., Quantitative analysis of the biomineralization of different hard tissue. *J. Microsc.*, 2001, **202**, 488–494.
12. Leng, Y., Chen, J. and Qu, S., TEM study of calcium phosphate precipitation on HA/TCP ceramics. *Biomaterials*, 2003, **24**, 2125–2131.
13. Brès, E. F., Hutchison, J. L., Senger, B., Voegel, J.-C. and Frank, R. M., HREM study of irradiation damage in human dental enamel crystals. *Ultramicroscopy*, 1991, **35**(34), 305–322.
14. Nicolopoulos, S., González-Calbet, J. M., Alonso, M. P., Gutierrez-Rios, M. T., de Frutos, M. I. and Vallet-Regi, M., Characterization by TEM of local crystalline changes during irradation damage of hydroxyapatite compounds. *J. Solid State Chem.*, 1995, **116**, 265–274.
15. Meldrum, A., Wang, L. M. and Ewing, R. C., Electron-irradiation-induced phase segregation in crystalline and amorphous apaptite: a TEM study. *Am. Mineral.*, 1997, **82**, 858–869.
16. Leng, Y. and Qu, S., TEM examination of single crystal hydroxyapatite diffraction. *J. Mater. Sci. Lett.*, 2002, **21**, 829–830.
17. Henning, P. A., Landa-Cánovas, A. R., Larsson, A.-K. and Lidin, S., Elucidation of the crystal structure of oxyapatite by high-resolution electron microscopy. *Acta Cryst.*, 1999, **B55**, 170–176.
18. Liou, Sz-C. and Chen, S.-Y., Transformation mechanism of different chemically precipitated apatitic precursors into β-tricalcium phosphate upon calcination. *Biomaterials*, 2002, **23**, 4541–4547.
19. Elliott, J. C., *Structure and Chemistry of the Apatites and Other Calcium Orthophosphates*. Elsevier, Amsterdam, 1994.
20. Rangavittal, N., Landa-Canovas, A. R., Gonzales-Calbet, J. M. and Vallet-Regi, M., Structural study and stability of hydroxyapatite and β-tricalcium phosphate: two important bioceramics. *J. Biomed. Mater. Res.*, 2000, **51**(4), 660–668.
21. Mathew, M. and Takagi, S., Structures of biological minerals in dental research. *J. Res. Natl. Inst. Stand. Technol.*, 2001, **106**, 1035–1044.
22. Calderin, L., Scott, M. J. and Rubio, A., Electronic and crystallographic structure of apatites. *Phys. Rev. B*, 2003, **67**, 1341061–1341067.